

## High resolution imaging of transitional cell carcinoma with optical coherence tomography: feasibility for the evaluation of bladder pathology

<sup>1</sup>C A JESSER, BS, <sup>2</sup>S A BOPPART, PhD, <sup>2</sup>C PITRIS, MS, <sup>3</sup>D L STAMPER, PhD, <sup>4</sup>G PETUR NIELSEN, MD, <sup>1</sup>M E BREZINSKI, MD, PhD and <sup>2</sup>J G FUJIMOTO, PhD

Departments of <sup>1</sup>Medicine and <sup>4</sup>Pathology, Massachusetts General Hospital, and Harvard Medical School, Boston, MA 02114, <sup>2</sup>Department of Electrical Engineering and Computer Science, and Research Laboratory for Electronics, Massachusetts Institute of Technology, Cambridge, MA 02139 and <sup>3</sup>King's College, Wilkes-Barre, PA, USA

**Abstract.** Significant challenges regarding patient morbidity and mortality remain in the management of transitional cell carcinoma (TCC). Among the most important of these challenges is the inability to identify early neoplastic changes and to assess the degree of tumour invasion into the bladder wall *in vivo*. Optical coherence tomography (OCT) has been recently developed to provide *in situ*, high resolution, catheter/endscope based imaging. This study explored the feasibility of OCT for the evaluation of bladder pathology. Both *in vitro* and *in vivo* studies were performed. *In vitro* imaging of pathological human bladder was performed and compared with normal specimens and histopathology. *In vivo* imaging of normal rabbit bladder was also performed with our current catheter/endscope based systems. In the *in vitro* studies, OCT was able to delineate normal microstructure of the bladder, such as the mucosa, submucosa and muscularis layers. This was in contrast to specimens of invasive carcinoma, where a disruption of the normal bladder wall architecture was seen. The *in vivo* experiment demonstrated current limitations of the catheter/endscope based systems and provided valuable information for developing an improved system for bladder imaging. The ability of OCT to delineate microstructure of the bladder wall suggests feasibility for endoscopic based imaging. In particular, there is a potential role envisioned for OCT in the management of TCC, identifying pre-malignant states and the depth of tumour invasion.

Although many aspects of the management of transitional cell carcinoma (TCC) are now well established, significant challenges remain that influence patient morbidity and mortality. Among the most important of these challenges is the inability to identify early neoplastic changes and to assess the degree of tumour invasion into the bladder wall [1]. For example, patients who have undergone local resection of superficial disease have recurrence rates as high as 60% [2]. Early detection and treatment of recurrent disease is required to maximize bladder preservation and patient survival [3]. However, current diagnostic methods have only a limited ability to detect early neoplastic lesions, such as carcinoma *in situ* and dysplasia, resulting in some patients presenting with invasive disease. Similarly, the optimal

management of patients with TCC requires that, during initial local staging, superficial tumours must be distinguished from those which have become invasive (T2). Once the tumour has spread into the muscular layer, both prognosis and therapy differ substantially from that of superficial disease [4]. During endoscopic evaluation the goal is to achieve accurate methods of assessing both the degree of tumour invasion and the presence of early neoplasia, thereby substantially improving patient management.

Cystoscopy, the direct visualization of the bladder surface via optical fibre bundles, is the current "gold standard" for the diagnosis of TCC [5]. Under cystoscopic evaluation, those tumours raised above the bladder surface can be readily detected. Furthermore, cystoscopy can be used to guide the transurethral resection of superficial tumours [3]. However, some clinically relevant pathology, which appears benign upon direct visualization, may go unobserved. This would include multiple site involvement at the time of local resection or the presence of recurrences

Received 1 March 1999 and in revised form 24 June 1999, accepted 8 July 1999.

Address correspondence to Dr Mark Brezinski, MD, PhD, Massachusetts Institute of Technology, Building 36-357, 50 Vassar Street, Cambridge, MA 02139, USA.

during subsequent screening. In addition, cystoscopy does not allow subsurface microstructural information to be obtained, such as the extent of tumour invasion into the bladder wall. Blind biopsy or cytology may be used in conjunction with cystoscopy, but they are of only limited value [6].

The limitations of cystoscopy have led investigators to examine other methods for interrogating the bladder wall. MRI, transabdominal ultrasound and CT are powerful imaging technologies for a wide range of medical applications, including the assessment of distant metastasis [4]. Unfortunately, their relatively low resolution ( $>500\ \mu\text{m}$ ) prevents assessments of microstructural changes within the bladder wall. High frequency endoscopic ultrasound (20 MHz) has been applied experimentally to the assessment of bladder carcinomas. However, its axial resolution of greater than  $150\ \mu\text{m}$  is also not sufficient for reliably identifying layers within the bladder wall, which has prevented its adoption into routine clinical use [7, 8]. Diffuse reflectance and fluorescence techniques have been explored, but high false positive rates have raised questions on their ultimate utility [9]. An imaging technology capable of assessing the bladder wall near the resolution of histopathology would be a powerful tool to overcome these limitations in the management of TCC.

Optical coherence tomography (OCT) is a recently developed technology which performs real-time, micron scale imaging ( $4\text{--}20\ \mu\text{m}$ ) near the level of histopathology [10]. OCT is analogous to ultrasound B-mode imaging, except that it uses infrared light as opposed to acoustical radiation. OCT performs two- and three-dimensional imaging in biological tissues by directing an optical beam onto the tissue and measuring the reflected or backscattered intensity of light as a function of depth. Thus, an OCT image represents a cross-sectional picture of the optical reflectance properties of the tissue, similar to acoustical reflectance imaging performed with ultrasound.

OCT was first applied to imaging the optically transparent structures of the eye [10]. When used in clinical practice, OCT has demonstrated significant promise in the detection and management of a variety of retinal diseases including glaucoma and macular oedema [11]. Recent advances have led to high resolution, real-time imaging of non-transparent tissue, such as the vascular system and gastrointestinal tract, through catheters and endoscopes [10, 12–14]. Pilot studies have also been performed *in vitro* on the urinary tract [15]. In non-transparent tissue, the penetration is approximately over the distance of a conventional biopsy ( $2\text{--}3\ \text{mm}$ ) at high resolution, which has led some investigators to term OCT imaging as optical biopsy. Direct

comparisons have been performed between OCT and the current clinical technology with the highest resolution, high frequency ultrasound (30 MHz). OCT demonstrated superior performance both quantitatively and qualitatively [16].

Several features, in addition to its high resolution, make OCT attractive for assessing bladder pathology. First, OCT technology is fibre optic based, which allows its relatively straightforward integration with small catheters/endoscopes. The current prototype OCT catheter/endoscope is 1 mm in diameter, but much smaller devices are possible with future modification. Second, unlike CT or MRI, OCT imaging is performed in real-time, allowing large amounts of information on bladder microstructure to be saved in sVHS or digital format. Third, OCT imaging is compact and portable, smaller than a standard ultrasound machine. Finally, as an optical imaging technology, OCT can be combined with other optical modalities such as absorption and polarization spectroscopy.

In this study, the feasibility of OCT for the evaluation of bladder pathology was assessed via *in vitro* studies on transitional cell tumours post-resection. The images were correlated with histology to confirm tissue identity. *In vivo* imaging performed on a normal rabbit bladder has also been included to demonstrate limitations in current catheter/endoscope based systems.

## Materials and methods

The principles behind OCT have been previously described [10, 12]. A schematic of the complete OCT system is shown in Figure 1. In OCT, low coherence light is directed at the sample and the light reflected from the various internal structures is detected. This is analogous to the use of sound waves in ultrasound to perform imaging. However, unlike ultrasound, the speed of light is very high, rendering direct electronic measurement of the echo delay time of the reflected light impossible. Therefore, a technique known as low coherence interferometry is used. With interferometry, the beam leaving the light source is split into two parts, a reference and a sample beam. The reference beam is reflected off a mirror at a known distance and returns to the detector. The sample beam reflects off different layers within the tissue and light returning from the sample and reference arms are recombined. Light that returns simultaneously to the detector from both arms, and therefore has travelled the same pathlength, interferes upon reaching the detector. OCT measures the intensity of this interference. The intensity of interference correlates with the intensity of backreflection. By changing the distance light travels in the reference arm, through

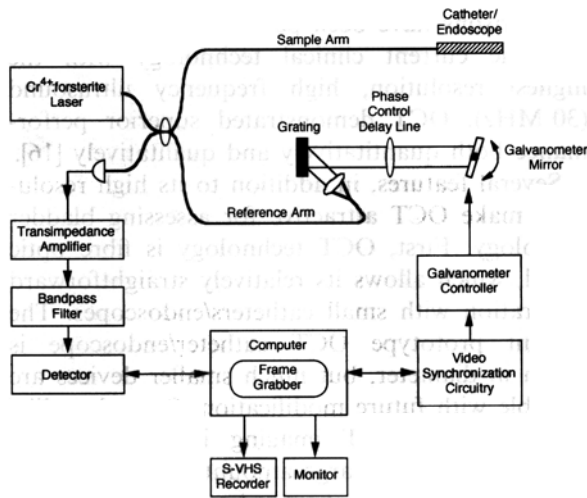


**Figure 1.** Schematic of the OCT instrument. OCT is analogous to ultrasound, measuring the intensity of backreflected infrared light rather than sound waves. Owing to the high speeds associated with the propagation of light, a technique known as low coherence interferometry is required to measure the echo time delay of backreflection. Interferometry and the use of a reference arm path are described in the text.

the use of a moving mirror which changes the optical pathlength in that arm, measurements of the intensity of interference can be obtained from different points within the tissue. Scanning the beam across the sample and recording the optical backscattering *versus* depth at different transverse positions produces two- or three-dimensional images.

The resolution is related to a property of the light source referred to as the bandwidth, which is the range of wavelengths within the beam. The relationship between optical bandwidth ( $\Delta\lambda$ ) and ranging resolution ( $\Delta L$ ) is well established by previous results and from electromagnetic theory and is given mathematically by the formula [17]:

$$\Delta L = \frac{2 \ln(2)}{\pi} \frac{\lambda^2}{\Delta\lambda}$$

In the *in vitro* experiments, the source used was a 1310 nm quantum well source (AFC, Hull, Qc, Canada) with a bandwidth of 45 nm. This corresponds to a measured axial resolution of 18  $\mu\text{m}$ . The lateral resolution is determined by the optical spot size which is related to numerical aperture of the focused beam (which also determines the depth of field or confocal parameter) similar to light microscopy. The lateral resolution was 30  $\mu\text{m}$ .

The measured signal-to-noise ratio (SNR) was above 100 dB, using a power of 3–4 mW at the sample. The SNR was measured by measuring the maximum signal when the optical beam was reflected from a high reflecting mirror divided by

the background noise level of the instrument. This SNR determines the dynamic range with which it is possible to image. In general, the SNR for this type of optical measurement can be predicted by using results from optical communications theory [18]. The SNR determines the minimum detectable reflectivity from the tissue and can be mathematically described by:

$$\text{SNR} = \frac{1}{2} \frac{\eta \cdot P_s}{\hbar\omega \cdot \text{NEB}}$$

where  $\eta$  is the detector quantum efficiency,  $\hbar\omega$  is the photon energy, NEB is the noise equivalent bandwidth of the demodulation filter, and  $P_s$  is the power received by the detector from the sample arm. The sensitivity to weakly reflected light depends only on the detection filter bandwidth and the available optical power.

Bladder tissue from human subjects was used for *in vitro* studies. Normal bladder tissue was obtained from autopsies of three patients. Abnormal bladder tissue was obtained following surgical resection from five patients. The tissue specimens were placed in a Petri dish and irrigated with isotonic saline to prevent dehydration during imaging. The acquisition of each *in vitro* image required between 10 and 40 s depending on the size (number of pixel elements) of the image. A total of 116 *in vitro* images was taken; 30 of the normal bladder samples and 86 of the abnormal samples. All imaging was performed between 1 and 4 h after obtaining the tissue. Since the OCT beam is invisible, tissue registration was performed with a visible light guiding beam. The orientation of the imaging scan was marked on the specimen using the microapplication of India ink. The samples then underwent routine histological processing. Samples were immersed in 10% buffered formalin for 48 h. The tissues were then processed for standard paraffin embedding. Five micron-thick sections were cut at the previously marked imaging sites and stained with hematoxylin and eosin (H&E). The stained histological sections enabled verification of tissue identity and in most instances allowed identification of sources of tissue contrast in the OCT images.

An *in vivo* imaging experiment was also performed on a normal rabbit bladder to evaluate current limitations of the catheter/endoscope based systems. This protocol has been approved by the Committee on Animal Care both at Massachusetts General Hospital and Massachusetts Institute of Technology. *In vivo* imaging was performed on a normal, 12-week-old New Zealand White rabbit. After the animal was anaesthetized, a 7 French Judkins catheter was introduced into the bladder as a guiding catheter to prevent damage to the OCT imaging

catheter/endscope. The 2.9 French, radial OCT imaging catheter/endscope was then introduced into the bladder through the guiding catheter. Imaging was performed at 4 frames per second at an axial resolution of 9.2  $\mu\text{m}$ . Data were saved in both sVHS and digital formats. After imaging, gross tissue registration was performed by suturing the guiding catheter in place. The animal was then sacrificed and the imaged regions were excised and immersed in 10% formalin in preparation for routine histological processing. The specimens were blocked in paraffin, cut into 5  $\mu\text{m}$  sections, and stained with H&E for microscopic examination.

A solid state laser, which generates pulses of femtosecond duration ( $\sim 10^{-15}$  s), was used for high speed, *in vivo* OCT imaging. Specifically, a Kerr-lens modelocked,  $\text{Cr}^{4+}$ :Forsterite laser was utilized which had a median wavelength of 1280 nm and a bandwidth of 75 nm. The transverse or lateral resolution is determined by the spot size or focusing power of the lens system and was measured to be 30  $\mu\text{m}$ . Acquisition rates were 4 frames per second for an image consisting of 512 transverse pixels. The high speed data acquisition system uses a phase delay device rather than a moving mirror to change the optical group delay in the reference arm. This device scans the phases of the different frequency components of the optical beam in the reference arm in order to vary the effective optical delay and permits extremely high data acquisition speeds to be achieved. The optical power incident on the sample was  $\sim 10$  mW. The SNR was 106 dB. A schematic and photograph of the OCT imaging catheter/endscope are shown in Figure 2. The catheter/endscope consisted of an encased, rotating speedometer cable carrying a single mode optical fibre. The beam is focused by a graded index (GRIN) lens and is directed by a microprism. The beam was scanned circumferentially by rotating the cable, fibre and optical assembly inside the static housing. The catheter/

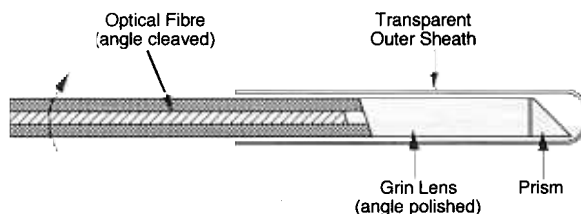


**Figure 2.** Schematic of the catheter/endscope. A radial imaging OCT catheter/endscope was used for assessments of the rabbit bladder *in vivo*. The catheter/endscope is 2.9 French or 1 mm in diameter. Imaging was performed at 4 frames per second at an axial resolution of 9.2  $\mu\text{m}$ . Data were saved in both sVHS and digital formats.

endscope featured a small diameter of  $\sim 1$  mm (2.9 F) and was optimized to reduce parasitic internal reflections. Power loss caused by suboptimal coupling and internal reflection within the catheter/endscope was 3–4 dB, but could be reduced by further optimization. The axial dimension (scan depth) of each OCT image was 2.3 mm which was digitized to 248 pixels. Imaging was performed with 512 transverse pixels (corresponding to different radial angles) with image acquisition times of 250 ms.

## Results

OCT images of normal bladder obtained from autopsy were taken and are shown in Figure 3. In the OCT images, the mucosa/submucosal interface (red arrow) as well as the submucosa/muscularis interface (black arrow) were differentiated (Figures 3A and C). High muscle bundles were seen (m). The corresponding histology (Figures 3B and D) was included.

Figure 4 also shows images of normal bladder. In Figure 4A, the mucosa/submucosa interface (yellow arrow) and submucosa/muscularis interface (blue arrow) were delineated. Vessels (v) were also noted within the wall. In Figure 4C, a section of bladder with relatively little mucosal layer was imaged. This section was included since it confirmed that the submucosa/muscularis layer on previous images was correctly identified. In Figures 4C and D capillaries within the submucosa were identified (red arrows).

Figures 5A and C are OCT images of invasive transitional cell carcinoma. The mucosa/submucosal and submucosal/muscularis boundaries were no longer clearly observed. In addition, no capillaries were noted, which were present in all normal images. There were distorted sections of muscle bundles in Figures 5A and B (red arrows). The OCT image in Figure 5A has also shown an area of fat (blue arrow) from the outer edge of the sample. In Figures 5B and D the structures of the tumours were confirmed by histopathology.

An *in vivo* image of the rabbit bladder and the corresponding histology are shown in Figure 6. The images were obtained at 4 frames per second through a 1 mm (diameter) OCT imaging catheter/endscope. Although the axial resolution was approximately the same as the *in vitro* system, the transverse resolution was greater than 50  $\mu\text{m}$ .

## Discussion

A technology capable of performing real-time, micron scale imaging of the bladder wall would be a powerful adjuvant to conventional endoscopy. In particular, this technology could potentially show greatest utility in the management of TCC,

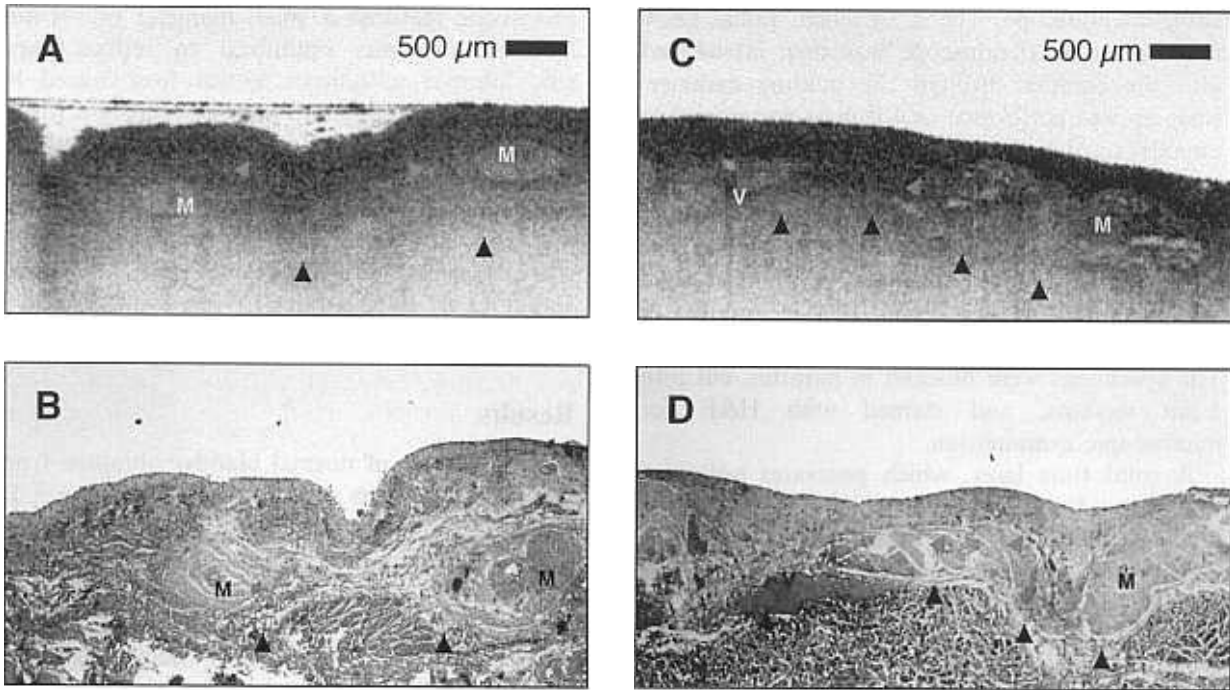


**Figure 3.** Normal bladder. OCT image of normal bladder and corresponding histology. (A, B, C, D) Mucosa/submucosal interface (red arrow) and submucosa/muscularis interface (black arrow) are identified. High muscle bundles (M) are noted. Bar represents 500  $\mu\text{m}$  in all OCT images. (B, D) Corresponding histology.

where the degree of tumour invasion and the presence of early neoplastic disease cannot currently be effectively characterized. In this study, the feasibility of OCT is demonstrated for high resolution assessment of the bladder. At 10  $\mu\text{m}$ , the resolution of OCT is higher than any clinical imaging technology. OCT was able to delineate normal microstructure of the bladder, such as vessels, and the mucosa, submucosa and muscularis layers. This was in contrast

to specimens of invasive carcinoma, where a disruption of the normal bladder wall architecture was seen.

The major limitations of this study were the accessible range of pathology and the performance of the *in vivo* imaging catheter/ endoscope. Samples examined in this study were obtained after surgical resection. All samples examined contained invasive disease. Pre-malignant states, such as carcinoma *in situ* or dysplasia,

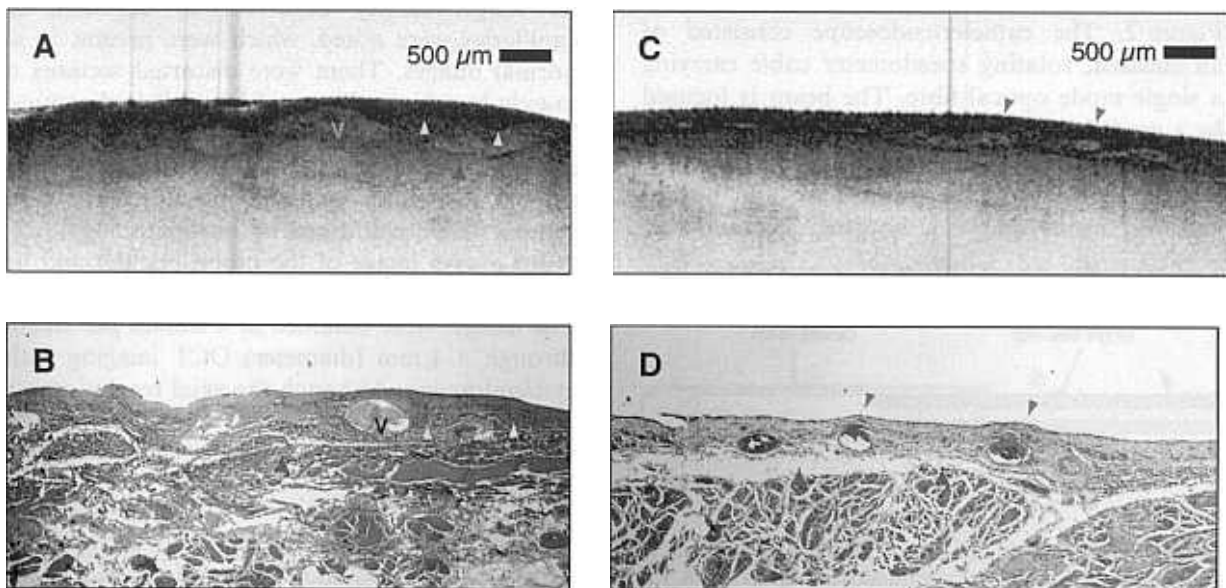


**Figure 4.** Normal bladder. OCT image of normal bladder and corresponding histology. (A, B) The mucosa/submucosa interface (yellow arrow) is delineated. (A, B, C, D) The submucosa/muscularis interface (blue arrow) is delineated. (A, B) Vessels (v) are noted within the wall. (C, D) A section of bladder with relatively little mucosal layer and capillaries within the submucosa (red arrow).

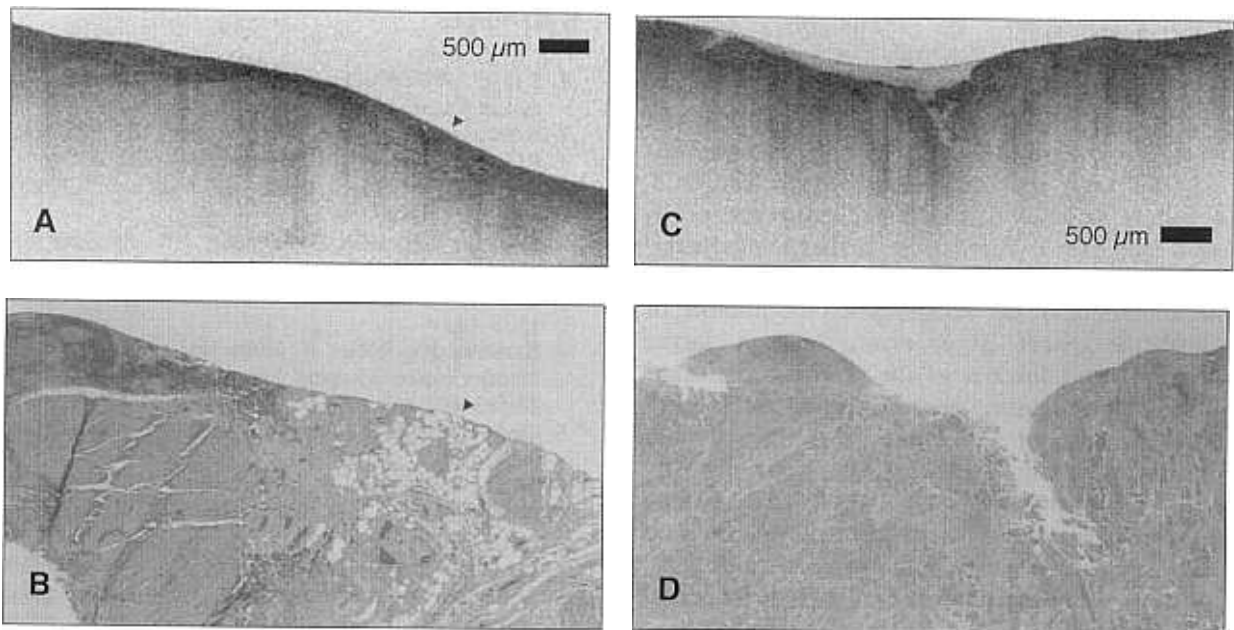


**Figure 5.** Transitional cell carcinoma. OCT images of invasive transitional cell carcinoma and corresponding histology. (A, C) Distinct layers, boundaries and capillaries are no longer observed that were present in all normal images. There are distorted sections of muscle bundles in (A) and (B) (red arrows). (A, B) An area of fat (blue arrow) from the outer edge of the sample is noted. (B, D) The structures of the tumours are confirmed by histopathology.

were unavailable. However, since delineation of individual layers within the wall was achieved with OCT in normal samples, it remains likely that OCT will be able to provide superior structure information about early neoplasia when compared with current technologies. Future studies will obviously need to confirm this hypothesis.

For *in vivo* imaging of the bladder, the low transverse resolution achieved with the OCT imaging emphasizes that redesign will be necessary. The 2.9 French imaging catheter/endscope was constructed for use in the oesophagus,

trachea and aorta, which are small circular structures. Two problems resulted when using this catheter/endscope in the bladder. First, since the bladder is a relatively large, irregularly shaped organ and the catheter/endscope was designed to have a fixed working distance (distance to point of focus), the bladder wall was predominantly displaced from the focal plane during imaging. This resulted in relatively low transverse resolutions. When performing a cross-sectional image in a small, circular organ such as the oesophagus or aorta, the distance from the catheter/endscope to the wall remains relatively constant as long as the

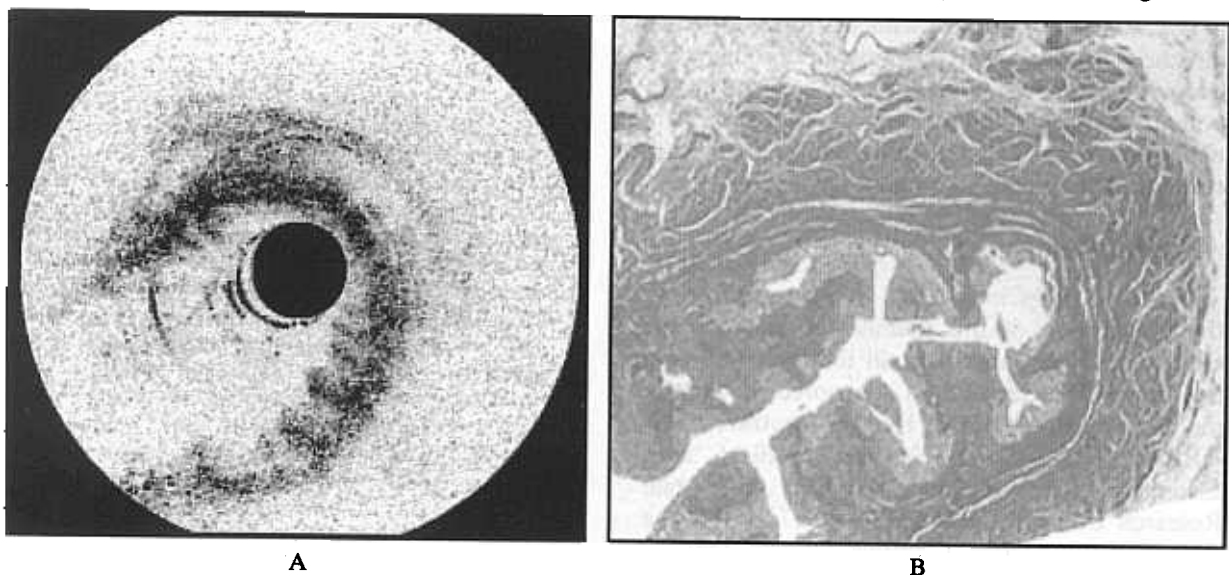


**Figure 6.** *In vivo* imaging of the bladder. (A) An *in vivo* image of the rabbit bladder and (B) the corresponding histology.

catheter/endscope is reasonably centred. Therefore, unlike the bladder, a radial imaging catheter/endscope with a fixed working distance can be used. The second problem, which resulted when using this catheter/endscope design, was that the pixel size was relatively large. The OCT system is designed to image 512 transverse pixels with each 360° rotation. The farther the catheter/endscope is from the wall, the greater the circumference of the image. Since the number of transverse pixels is constant, over a larger circumference, the size of the pixel has increased (effectively decreasing lateral imaging resolution). Both of these problems can be addressed with catheter/endscope redesign. In particular, by using a forward rather than transverse imaging catheter/endscope, the working distance and pixel size can be controlled and kept small.

Future engineering efforts will include increased data acquisition rates and increased resolution. The data acquisition rates were a maximum of 4 frames per second during this study. Future advances will likely result in video rate improvements. The ability to identify individual cells and assess subcellular structures such as the nuclei would also likely be of value in the evaluation of transitional cell carcinoma. Recently, solid state lasers have been used for OCT imaging which achieve resolutions of less than 4 µm, allowing true subcellular imaging to be achieved in living organisms [19]. Although these sources are complex and not viable for a clinical instrument, robust sources with similar bandwidth characteristics will probably be available in the near future. Therefore, subcellular *in vivo* imaging is a possibility for future clinical OCT systems.

## Conclusion

The ability of OCT to delineate microstructure of the bladder wall suggests feasibility for endoscopic based imaging. In particular, a potential role is envisioned for OCT in the management of TCC, identifying pre-malignant states and the depth of tumour invasion.

## Acknowledgments

We thank Ms Cindy Kopf for her assistance in the preparation of this manuscript and Mr Joe Gamba and Mr James Taralli for their technical assistance. This research is sponsored in part by the National Institutes of Health, Contract NIH-9-R01-EY11289-10 (JGF), the Medical Free Electron Laser Program, Office of Naval Research Contract N00014-94-1-0717 (JGF), the Whitaker Foundation Contract 96-0205 (MEB), 1R01AR44812-01 (MEB), and the National Institutes of Health, Contract NIH-1-R29-HL55686-01A1 (MEB).

## References

1. Kryger JV, Messing E. Bladder cancer screening. *Semin Oncol* 1996;23:585-97.
2. Kiemeny LA, Witjes JA, Verbeek AL, Heijbroek RP, Debruyne FM. The clinical epidemiology of superficial bladder cancer. *Br J Cancer* 1993;67:806-12.
3. Fleshner NE, Herr HW, Stuart AK, Murphy GP, Mettlin C, Menck HR. The national cancer data base report on bladder carcinoma. *Cancer* 1996;78:1505-13.
4. Barentsz JO, Witjes A, Ruijs JHJ. What is new in bladder cancer imaging. *Urol Clin North Am* 1997;24:583-602.
5. Ozen H. Bladder cancer. *Current Opin Oncol* 1997;9:295-300.
6. Walsh P, Gittes R, Perlmutter A, Stamey T. *Campbell's urology*. Philadelphia: WB Saunders, 1981:1374.
7. Liu JB, Bagley DH, Conlin MJ, Merton DA, Alexander AA, Goldberg BB. Endoluminal sonographic evaluation of ureteral and renal pelvic neoplasms. *J Ultrasound Med* 1997;16:515-21.
8. Koraitim M, Kamal B, Metwalli N, Zaky Y. Transurethral ultrasonographic assessments of bladder carcinoma: its value and limitation. *J Urol* 1995;154:375-8.
9. Koenig F, McGovern FJ, Enquist H, Larne R, Deutsch TF, Schomacker KT. Autofluorescence guided biopsy for the early diagnosis of bladder carcinoma. *J Urol* 1998;159:1871-5.
10. Huang D, Swanson EA, Lin CP, Schuman J, Stinson WG, Chang W, et al. Optical coherence tomography. *Science* 1991;254:1178-81.
11. Puliafito CA, Hee MR, Schumman JS, Fujimoto JG. Optical coherence tomography of ocular disease. Thorofare, NJ: SLACK Inc., 1995.
12. Brezinski ME, Tearney GJ, Bouma BE, Izzat JA, Hee MR, Swanson EA, et al. Optical coherence tomography for optical biopsy: properties and demonstration of vascular pathology. *Circulation* 1996;93:1206-13.
13. Fujimoto JG, Brezinski ME, Tearney GJ, Boppart SA, Bouma BE, Hee MR, et al. Optical biopsy and imaging using optical coherence tomography. *Nat Med* 1995;1:970-2.
14. Tearney GJ, Brezinski ME, Bouma BE, Boppart SA, Pitris C, Southern JF, et al. *In vivo* endoscopic optical biopsy with optical coherence tomography. *Science* 1997;276:2037-9.
15. Tearney GJ, Brezinski ME, Southern JF, Bouma BE, Boppart SA, Fujimoto JG. Optical biopsy in human urologic tissue using optical coherence tomography. *J Urol* 1997;157:1915-9.
16. Brezinski ME, Tearney GJ, Weissman NJ, Boppart SA, Bouma BE, Hee MR, et al. Assessing atherosclerotic plaque morphology: comparison of optical coherence tomography and high frequency intravascular ultrasound. *Heart* 1997;77:397-404.
17. Swanson EA, Huang D, Hee MR, Fujimoto JG, Lin CP, Puliafito CA. High-speed optical coherence domain reflectometry. *Opt Lett* 1992;17:151-3.
18. Saleh B, Teich M. *Fundamentals of photonics*. New York, NY: Wiley, 1991.
19. Boppart SA, Bouma BE, Pitris C, Southern JF, Brezinski ME, Fujimoto JG. *In vivo* cellular optical coherence tomography imaging. *Nat Med* 1998;4:861-5.